NASA/TM—1999-209377

SAE 99–01–2431

Analysis of Direct Solar Illumination on the Backside of Space Station Solar Cells

Ann M. Delleur and Thomas W. Kerslake
Glenn Research Center, Cleveland, Ohio

David A. Scheiman
Ohio Aerospace Institute, Cleveland, Ohio

Prepared for the
34th Intersociety Energy Conversion Engineering Conference
sponsored by the Society of Automotive Engineers
Vancouver, British Columbia, Canada, August 1–5, 1999

National Aeronautics and
Space Administration

Glenn Research Center

July 1999

Acknowledgments

The authors wish to thank Mr. Jeffrey S. Hojnicki of GRC for his assistance to the authors with code development; Mr. James Fincannon of GRC for his assistance with the shadowing model; Mr. Michael Klamph of the MAGIK team for his analysis of array lock angle envelopes for the PV module installation procedure; and both Lockheed Martin's SEMDA lab, and the JSC's MAGIK team for use of their detailed graphics.

Available from

NASA Center for Aerospace Information
7121 Standard Drive
Hanover, MD 21076
Price Code: A03

National Technical Information Service
5285 Port Royal Road
Springfield, VA 22100
Price Code: A03

Analysis of Direct Solar Illumination on the Backside of Space Station Solar Cells

Ann M. Delleur and Thomas W. Kerslake
NASA Glenn Research Center
Cleveland, Ohio 44135

David A. Scheiman
Ohio Aerospace Institute
Cleveland, Ohio 44142

ABSTRACT

The International Space Station (ISS) is a complex spacecraft that will take several years to assemble in orbit. During many of the assembly and maintenance procedures, the space station's large solar arrays must be locked, which can significantly reduce power generation. To date, power generation analyses have not included power generation from the backside of the solar cells in a desire to produce a conservative analysis. This paper describes the testing of ISS solar cell backside power generation, analytical modeling, and analysis results on an ISS assembly mission.

INTRODUCTION

It will take several years to complete the multifarious assembly of the ISS in orbit. During ISS procedures such as solar array installation, maintenance operations, docking and separation with the space shuttle or other spacecraft, the solar arrays are locked. This accommodates astronaut access or orients the arrays to reduce thruster plume forces on the arrays by docking and undocking spacecraft.

When the arrays are locked and unable to track the sun, power production is significantly reduced. Often the backside of the array will face the sun for some portion of the orbit, under these conditions. Since the solar cells are mounted on a thin, solar transparent substrate, appreciable power is produced under backside illumination. To date, analyses have not included this backside power generation due to a desire to produce a conservative analysis. However, the extra power from backside generation could be very beneficial under restricted array pointing conditions, especially during power-intensive extravehicular activity.

To provide a more detailed assessment of the ISS power production capability, engineers at the NASA Glenn Research Center (GRC) measured the performance of backside direct solar illumination of ISS solar cells and incorporated this data in the energy balance analyses of several ISS assembly missions. This paper describes the methods used to measure solar cell backside response and model ISS solar array performance during back illumination. Analyses were performed using SPACE, a NASA/GRC developed computer code for the ISS program office [1].

METHODS

Quantifying the impact of backside power generation was performed in three stages: 1) lab measurement of the front and backside of the cell under controlled conditions, 2) normalization of the data, and 3) analytical modeling of the backside cell response to direct solar illumination.

TEST ARTICLE

A coupon, of 10 series-connected ISS solar cells, was used as the test article. The ISS solar cell is a 8 cm x 8 cm x 200 μm, n-on-p, crystalline silicon cell with a 125 μm borosilicate cover glass. The solar cells are mounted to a 125 μm thick, composite polyimide / glass scrim cloth / silicone adhesive substrate. The cells are interconnected via a 37 μm thick, flat copper conductors welded to contacts on the back of the solar cells. These copper conductors cover approximately 31% of the solar cell's 62.2 cm^2 area. To collect coupon electrical data, test wires were soldered to exposed flat copper interconnect conductors. The coupon was mounted on a pivot arm and electrically isolated to avoid ground-loop currents.

MEASUREMENT OF BACKSIDE POWER GENERATION

The first step required a quantification of the power generation from the backside of the solar cells. The 10-cell test coupon was used to collect electrical performance data by standard flash testing. Flash test equipment included a Spectrolab Inc. Large Area Pulsed Solar Simulator (LAPSS100) Xenon flash source, a monitor cell, an airplane standard cell, an ISAAC 2000 data acquisition system, and a PC. The typical LAPSS flash intensity ramped up very quickly, fell off slightly,

and then remained flat (<5% variation) for as much as 2 milliseconds, then tapered off exponentially. The monitor cell was kept at a short circuit to monitor the intensity of the light as a function of time (solar cell short circuit current varies linearly with intensity). Monitor cell current was used to correct for the <5% variation in flash intensity and to trigger a load voltage ramp circuit during the flat portion of the flash. The ramp started from 0 V and went to the open circuit voltage of the 10-cell coupon. High speed data acquisition circuitry recorded up to 150 sets of simultaneous voltage, current (measured voltage across a shunt resistor), and monitor current measurements during the ramp. All voltage measurements were made using the "4-wire" technique to eliminate test wire voltage drops. The data acquisition system simultaneously read the three data channels with 12 bit accuracy at a frequency of 150 kHz. An airplane calibrated standard solar cell was used to adjust the flash intensity to simulate air mass zero, 1-sun illumination conditions.

The 10-cell coupon was flash tested on the front side (with solar cells) and on the backside (solar cell substrate). Care was taken to eliminate spurious reflected light onto the coupon. Black paper was positioned behind the coupon and on the floor in front of the coupon, while black curtains were positioned between the LAPSS and the coupon. During testing, laboratory lights were turned off. The 0.165 m wide coupon was located 6.4 m from the LAPSS. The coupon was manually rotated via the pivot arm from 0° (normal incidence on the front) to 180° (normal incidence on the back) at 10° increments with respect to the fixed flash light source. At each angle of illumination incidence, the coupon was tested with a 1-millisecond flash duration and the current-voltage (IV) curve was measured. Tests were performed twice at each angle to ensure data consistency and repeatability. When oriented edge-on to the light source, the illumination intensity varied ±3% over the width of the coupon due to distance effects. Other experimental uncertainties and errors included: coupon angular position accuracy (±2°), coupon flatness (±2°), flash spatial uniformity (±2%), flash temporal uniformity (±2%), and coupon temperature variation (±1°C). At normal angle of incidence, the coupon IV curve was measured for flash durations of 1 millisecond and 1.75 milliseconds to assess capacitive effects. Based on these data, the capacitive measurement error in cell current and voltage was determined to be -0.1% to -1.2%.

DATA

Average coupon cell IV properties of the front side were determined, via flash testing, to be: 2.651 A short-circuit current (Isc), 0.691 V open-circuit voltage (Voc), 2.417 A maximum power current (Imp), 0.475 V maximum power voltage (Vmp), 1.149 W maximum power (Pmp), and a 0.700 fill factor (FF) at a cell temperature of 22.4°C. As the illumination angle of incidence varies, cell IV properties change due to projected area loss, cover glass Fresnel reflection, edge effects (light collection, scattering, and refraction), shadowing, and other effects [2]. Projected area loss is the primary contributor to cell performance changes up to incidence angles of about 60°. Above 60°, the other mechanisms affecting cell performance become significant.

Normalized cell IV performance data versus angle of incidence are plotted in Figure 1, for the front side, and in Figure 2, for the backside. Cell IV properties were normalized by those obtained with normal incidence front side illumination. Cell currents decreased with the cosine of the illumination incidence angle up to 60°. Above 60°, current losses greater than projected area loss resulted as a consequence of edge effects. Consistent with cell electrical theory [2], the normalized open-circuit voltage, Voc*, varied according to the relationship:

$$Voc^* = Voc_\alpha / Voc_0 = \ln (Isc_\alpha / Io) / \ln (Isc_0 / Io) \qquad (1)$$

Isc = short circuit current
Io = cell diode saturation current, 5.8E-09 A
Voc_α = open-circuit voltage at α angle of incidence
Voc_0 = open-circuit voltage at 0° angle of incidence
Voc* = normalized open-circuit voltage

Also consistent with cell electrical theory, the Vmp increased with decreased effective illumination from off-pointing and/or polyimide substrate transmission losses. This effect was most pronounced in the backside data set (Figure 2) where the normalized Vmp was above 1.0 over a wide range of incidence angles. Two noteworthy observations from this data set were: (1) the back-illuminated cells produced 41% as much power as the front-illuminated cells and (2) under edge illumination, the cells produced ~70% of the voltage attained with normal front side illumination.

ANALYTICAL MODELING

Exponential Model

Cell IV performance under back illumination was modeled almost identically to that under front illumination: that is, the cell current, I, as a function of operating voltage, V, was represented by a single exponential function [2]:

$$I = Isc - Io^*[\exp\{q^*(V-I^*Rs)/\gamma^*k^*T\}-1] - V / Rsh \qquad (2)$$

γ = curve fitting parameter
I = cell current
k = Boltzmann constant
Io = cell diode saturation current, 5.8E-09 A
q = an electron unit charge
Rs = cell series resistance
Rsh = cell shunt resistance
T = cell absolute temperature
V = cell voltage

The cell shunt resistance is assumed to be very large so that the V/Rsh term vanishes. The unknown terms of this equation, Io, Rs, and γ were determined based on the instantaneous values of cell Isc, Voc, Imp, and Vmp. Instantaneous values were based on cell age, degradation factors, operating temperature, and solar pointing conditions. For the given backside solar off pointing angle, cell IV properties were obtained by first linearly interpolating normalized laboratory flash data (discussed above). These normalized properties were then multiplied by the instantaneous cell IV properties predicted for normal, front illumination.

Bilinear Model

The single exponential solar cell IV function can only be used within an envelope of cell IV properties. This envelope is shown in Figure 3. Instantaneous cell Imp/Isc and Vmp/Voc ratios must lie between the upper and lower curves, or the single exponential function can not be used. For atypical situations with very cold cell operating temperatures and/or weak solar illumination, cell current and voltage ratios lie outside of the acceptable envelope. For these cases, current and voltage ratios approached 1.0 so a bilinear function was used to approximate the cell IV response. Cell current was modeled as linear functions of operating voltage over the ranges from 0 to Vmp and from Vmp to Voc.

Limitations

The backside illumination modeling accounts for direct solar illumination, but does not take into account incident energy from other sources such as Earth albedo, spacecraft albedo, and Lunar albedo. Orbital performance data and analyses have shown that illumination of the backside from these other sources will not produce sizable power compared with direct solar illumination [3]. Since degradation mechanisms change cell IV properties, the input data used in this analytical model are strictly valid for beginning-of-life cell operation only. However, it has been shown that cell radiation damage, the predominant degradation factor, reduces the cell backside spectral response by only ~10% at a 1 MeV electron fluence of 1.5E+13 [4]. This is the equivalent radiation dose accumulated after 11.6 years of orbital operation. Thus, the normalized cell input data should be applicable for analytical predictions throughout the 10-year operating life of the ISS.

ANALYSIS APPLICATIONS

The ISS solar arrays track the sun during nominal operations. However, during maintenance procedures and assembly operations such as replacing a battery, or installing an additional solar array module, the solar arrays must be locked to accommodate clearance and access. During these procedures, the backside of the solar array can receive direct solar illumination.

SPACE, an integrated end-to-end computer code, was used to assess the impact of backside power generation on the ISS Electrical Power System (EPS) [1]. SPACE can be used for in either of two types of analyses that exercise solar cell modeling [6-8]:

- A *"source driven"* analysis which determines EPS capability, given orbit conditions, EPS configuration, EPS component ages, photovoltaic (PV) array pointing conditions, etc.
- A *"load driven"* analysis which analyzes the ability of the EPS to supply a given load demand.

SPACE can also be used for a *"point only"* analysis which accesses only the orbit mechanics, solar array pointing, shadowing, and geometry routines.

The backside cell model was incorporated into SPACE such that it operated in both the source driven and load driven analysis modes. Both the load driven and source drive models were used for the example analyses presented in this paper.

The shadowing algorithm was modified to calculate shadowing on both the front and backsides of the arrays.

To assess the impact of direct backside illumination, a case was needed that incorporated procedures that locked one or more PV arrays for upwards of an hour.

The assembly mission on which the third solar array module, or PV module, was selected. The third PV module is relocated during this assembly procedure from its initial location on top of the Z1 truss (Figure 4) to its final location, outboard on the port side (Figure 5). To accomplish this procedure, the PV module will be lifted off the Z1 truss with the Space Station Remote Manipulator System (SSRMS) or arm, then the arm and PV module will be translated by the Mobile Transporter (MT) to just in front of the inboard PV module. The arm will then reach across the inboard PV module to the far side, and attach what will then become the port outboard PV module.

As shown in Figure 6, in order for the arm to reach across the inboard PV module, one of the inboard PV module arrays must be locked, such that the array can not rotate in any axis. The range of possible lock positions for this array was determined by the robotic operations team, MAGIK, to accommodate both adequate clearance for the arm to reach across, as well as clear fields of view for the cameras that will be used to control the arm. While the inboard PV module array is locked, the power generation from this array can be substantially reduced by off-pointing and edge effects.

From the range of possible lock positions for the inboard PV module array, the angle that provided the best power on the front side of the array, at the given orbit conditions for this analysis, was selected. Even with this lock angle selection, the backside of the array saw the sun for the first half of the sunlit portion of each orbit, and the font side of the array saw the sun for second half of the sunlit portion of each orbit.

Past analyses of this installation procedure have shown that, with only front side illumination, the port inboard PV module array produced insufficient power to support the time-phase channelized load demand. The most recent analysis, performed for the Design Analysis Cycle 7 Issue Resolution (March 1999), used mission specific orbit parameters supplied by both the Johnson Space Center's (JSC) guidance, navigation, and control team and the loads and dynamics team. The orbit parameters included: the solar β angle (the angle between the Earth-sun line and the orbit plane), the ISS torque equilibrium attitude (TEA), altitude, etc.

This analysis used a solar β angle of ~0°. Further analysis showed that either very high negative or very high positive solar β angles yielded much lower battery depth of discharge (DOD) for the installation procedure. Also this analysis maintained a constant ISS attitude. During the PV module installation, the station will be in free drift with the attitude control system disengaged. The station is to drift inside the attitude envelope. If the station exits the attitude envelope, the SSRMS will be locked, the attitude control system enabled, and the station returned to its desired TEA. After the desired

TEA is obtained, free drift will be resumed. Within the array lock envelope, the array power was most sensitive to changes in pitch.

The analysis of the PV module relocation procedure was performed with only front side power generation and then the analysis was repeated with power generation from both the front and backside. All other inputs were identical between analyses.

The second example analysis was of the ISS stage 5A (Figure 7) in a tumbling scenario with both arrays locked. The objective was to determine if in a tumbling scenario, given random initial forces, if the backside illumination would provide a significant contribution to the array power.

RESULTS AND DISCUSSION

Figure 8, shows the array power generation in kW for only the front side of the locked array and the corresponding battery DOD for the applied load demand during eight orbital periods. The array tracked in one axis during the first insolation period; and thus the array power was nearly a square wave. For the next four orbits, the array was locked, producing a sine wave type of response for the array power generation. The array tracked the sun, again in one axis, for the last three orbits.

From the DOD in this figure, the batteries were discharged during eclipse to meet the load demand; however, the batteries did not return to full charge by the beginning of eclipse. The power generated from the array will be first used to meet the applied load demand, and then the remaining power will be used to charge the batteries. In this case, there was insufficient power to fully charge the batteries; thus the batteries began the third eclipse with 18.2% DOD. This situation was perpetuated for the next three orbits. The battery DOD increased until the batteries become almost fully discharged with a DOD of 95.6% by the end of the sixth orbit. If the array had remained locked beyond the sixth orbit, the DOD would have reached 100% and the applied load demand could not have been met.

Figure 9 shows the results of the same case, which includes backside power generation in the array power. The corresponding battery DOD is also presented.

The array power, Figure 9, displayed two distinct peaks per orbit while the array was locked. The first, and lower peak, was the power generation from direct solar illumination of the backside of the array for the first half of orbit insolation, and the second peak, was the front side power generation during the second half of orbit insolation. The front side peak was the same as in Figure 8.

The backside array response was similar to the front side in that it took the form of a sine wave but with only about 40% of the amplitude of the front side. The array, with the inclusion of both front and backside power generation, was able to produce sufficient power to meet the load demand and almost fully recharge the batteries, to a near zero battery DOD at the end of each orbit.

The maximum battery DOD for the front side during this assembly procedure reached 95.6%, while inclusion of power generated from the backside of the array kept the maximum DOD to 28.1%.

The purpose of this first analysis comparison was to determine if additional power generation from the backside of the arrays could, in a locked array condition, without significant solar off-pointing errors, build a power margin that would help make the assembly procedure viable.

The high battery DOD reached with only the front side is considered unacceptable to conduct this assembly procedure. Without inclusion of the backside power, this procedure would require extensive rework. Reworks could include, decreasing the loads on the channel, if possible; switching the loads to other channels; and/or restricting assembly procedure to a more favorable solar β angle range.

The second example, the stage 5A tumbling scenario, produced additional power as expected from the backside analysis. Figure 10 depicts the array power production for the front side of just one array during the tumbling scenario of 6 orbits. The front side of the array did not face the sun during the first orbit period and thus no power was produced. In Figure 11, the same scenario was rerun, this time with the backside power generation algorithm applied. The additional peaks from the backside were quite prominent, such as the time period from 35 to 90 minutes. The saw-tooth features in these curves reflected localized power losses due to transient shadows.

CONCULSION

Using test data and an empirical/analytical solar cell electrical model, ISS array power performance was predicted for back-illuminated operating conditions. This backside power generation could be used as margin or to resolve problems with operational power shortfalls. The decision of how to use this latent power generation capability ultimately rests with the ISS Program Office and ISS Mission Operation Specialists.

ACRONYMS

DOD:
Depth of Discharge
EPS:
Electrical Power System
GRC:
NASA John H. Glenn Research Center at Lewis Field
ISS:
International Space Station
JSC:
NASA Lyndon B. Johnson Space Center
LAPSS:
Large Area Pulsed Solar Simulator
MAGIK:
Manipulator Analysis, Graphics, and Integrated Kinematics
PV:
Photovolataic

SEMDA:
Systems engineering and Modeling and Design Analysis Laboratory
SSRMS:
Space Station Remote Manipulator System.
TEA:
Torque Equilibrium Attitude

CONTACT

Ann M. Delleur
NASA Glenn Research Center, MS 500-203
21000 Brookpark Road, Cleveland, OH 44135
Phone (216) 433-5519, Fax: (216) 433-2995
Email: ann.m.delleur@grc.nasa.gov

REFERENCES

1. Hojnicki, Jeffrey S., Green, Robert D., Kerslake, Thomas W., McKissock, David B., and Trudell, Jeffrey J., "Space Station Freedom electrical Performance Model," NASA Technical Memorandum 106395, 28th IECEC, Atlanta, Georgia, August 1993.
2. Burger, Dale R. and Mueler, Robert L., "Solar Cell Angle of Incidence Corrections," NASA Lewis Research Center, Proceedings of the 14th Space Photovoltaic Research and Technology 1995, Feb 01, 1996, p. 168-177.
3. Josephs, R. H., "Solar Cell Array Design Handbook," NASA CR-149364, Oct 1976.
4. Kerslake, Thomas W., and Hoffman, David J., "*Mir* Cooperative Solar Array Flight Performance and Computational Analysis," 32nd Intersociety Energy Conversion Engineering Conference Proceedings, paper no. 97235, Honolulu, Hawaii, Aug 1997.
5. Lillington, D. L., et al., "Optimization of Silicon 8cm x 8cm Wrapthrough Space Station Cells for 'On Orbit' Operation," IEEE 20th Photovoltaic Specialists Conference, Las Vegas, NV, Sept. 26-30, 1988, Vol. 2, p. 934-939.
6. Fincannon, J., Hojnicki, J.S., Garner, J.C., "Effects of Solar Array Shadowing on the Power capability of the Interim Control Module," 34th Intersociety Energy Conversion Engineering Conference Proceedings, paper no. IECEC99-77, Vancouver, B.C., Canada, August 1999.
7. Fincannon, J., Delleur, A., Green, R., Hojnicki, J., "Load Following Power Timeline Analysis for the International Space Station," NASA TM-107263, 31st Intersociety Energy Conversion Engineering Conference Proceedings, Washington, D.C, Aug 1996.
8. Fincannon, J., "Analysis of Shadowing Effects on Spacecraft Power Systems," NASA TM-106994, Fourth European Space Power Conference, Poitiers, France, September 4-8, 1995.

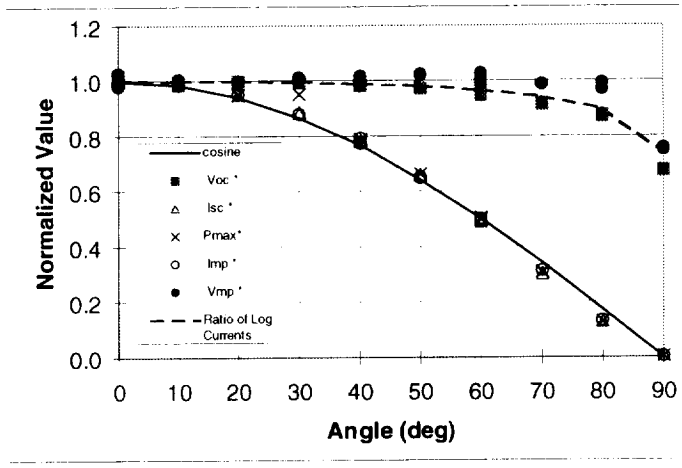

Figure 1. Normalized Cell Current Voltage Response versus Front Illumination Incidence Angle

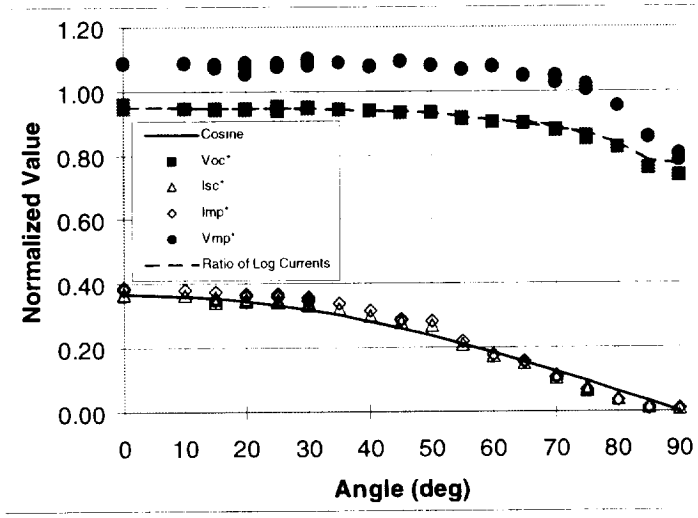

Figure 2. Normalized Cell Current Voltage Response versus Back Illumination Incidence Angle

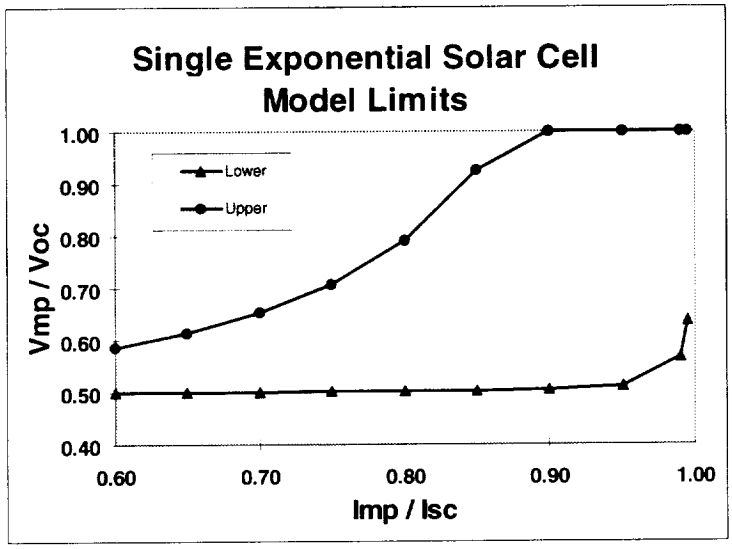

Figure 3. Single Exponential Solar Cell Model Limits

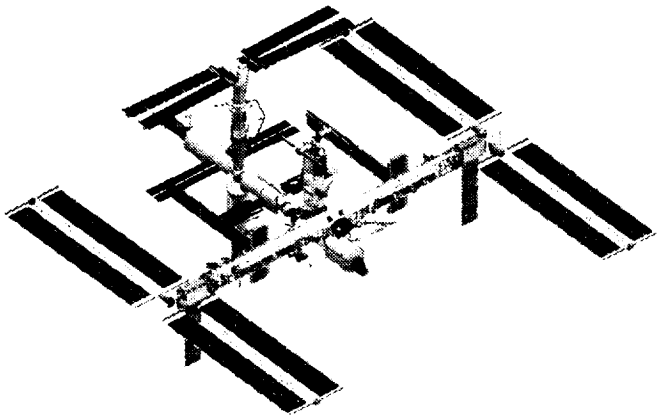

Figure 4. ISS before PV Module Relocation

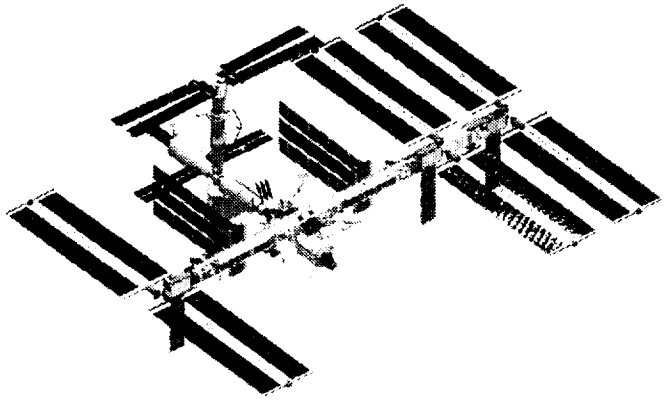

Figure 5. ISS after PV Module Relocation

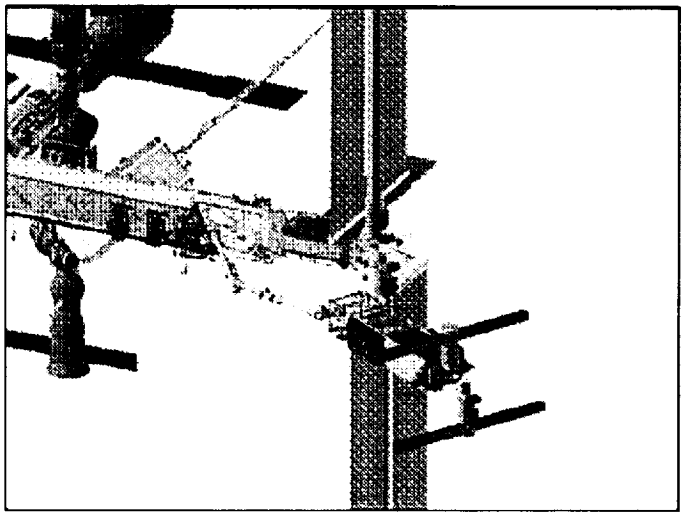

Figure 6. SSRMS moving the port outboard PV module into position for installation

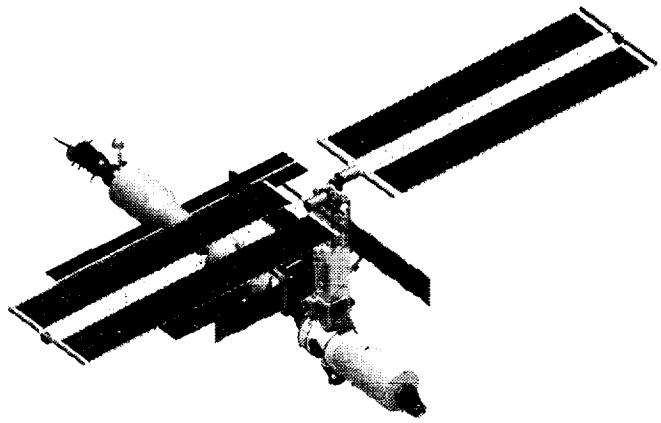

Figure 7. ISS Stage 5A

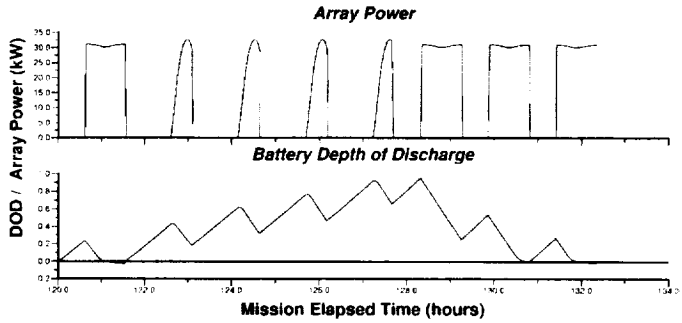

Figure 8. Front Side Array Power and DOD

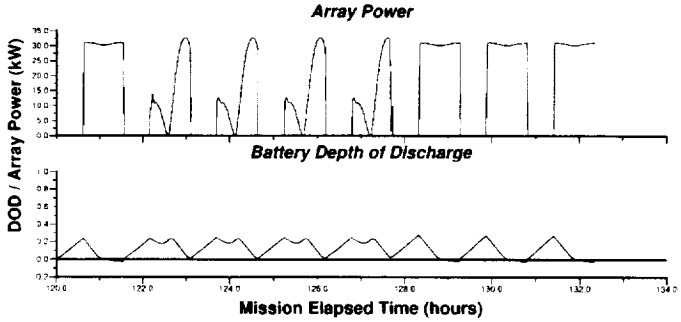

Figure 9. Combined front and backside array power and battery depth of discharge

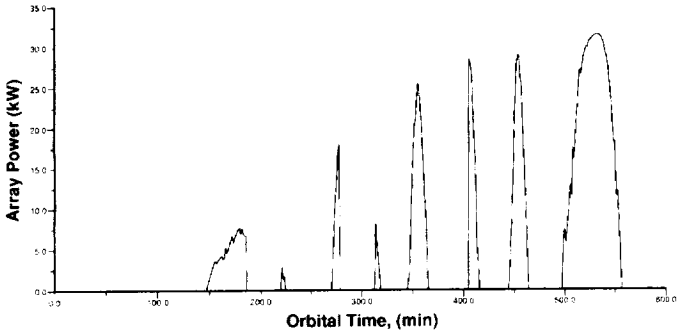

Figure 10. ISS Stage 5A Tumbling Front Side Array Power

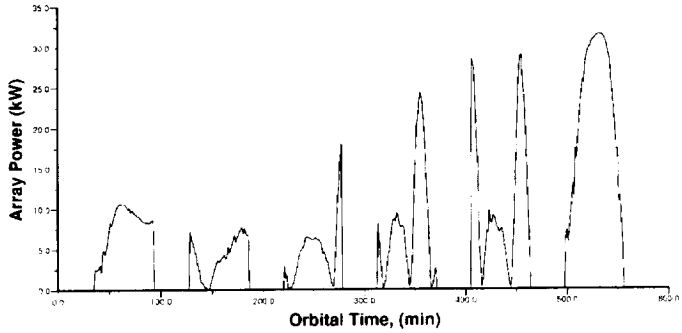

Figure 11. ISS Stage 5A Tumbling Combined Front and Backside Array Power

REPORT DOCUMENTATION PAGE

Form Approved
OMB No. 0704-0188

1. AGENCY USE ONLY (*Leave blank*)	2. REPORT DATE	3. REPORT TYPE AND DATES COVERED
	July 1999	Technical Memorandum

4. TITLE AND SUBTITLE

Analysis of Direct Solar Illumination on the Backside of Space Station Solar Cells

5. FUNDING NUMBERS

WU-575-15-69-00

6. AUTHOR(S)

Ann M. Delleur, Thomas W. Kerslake and David A. Scheiman

7. PERFORMING ORGANIZATION NAME(S) AND ADDRESS(ES)

National Aeronautics and Space Administration
John H. Glenn Research Center at Lewis Field
Cleveland, Ohio 44135-3191

8. PERFORMING ORGANIZATION REPORT NUMBER

E-11791

9. SPONSORING/MONITORING AGENCY NAME(S) AND ADDRESS(ES)

National Aeronautics and Space Administration
Washington, DC 20546-0001

10. SPONSORING/MONITORING AGENCY REPORT NUMBER

NASA TM—1999-209377
SAE 99-01-2431

11. SUPPLEMENTARY NOTES

Prepared for the 34th Intersociety Energy Conversion Engineering Conference sponsored by the Society of Automotive Engineers, Vancouver, British Columbia, Canada, August 1–5, 1999. Ann M. Delleur and Thomas W. Kerlsake, NASA Glenn Research Center, and David A. Scheiman, Ohio Aerospace Institute, 22800 Cedar Point Road, Cleveland, Ohio 44142. Responsible person, Ann M. Delleur, organization code 6920, (216) 433–5519.

12a. DISTRIBUTION/AVAILABILITY STATEMENT

Unclassified - Unlimited
Subject Category: 20 Distribution: Nonstandard

This publication is available from the NASA Center for AeroSpace Information, (301) 621–0390.

12b. DISTRIBUTION CODE

13. ABSTRACT ***(Maximum 200 words)***

The International Space Station (ISS) is a complex spacecraft that will take several years to assemble in orbit. During many of the assembly and maintenance procedures, the space stations's large solar arrays must be locked, which can significantly reduce power generation. To date, power generation analyses have not included power generation from the backside of the solar cells in a desire to produce a conservative analysis. This paper describes the testing of ISS solar cell backside power generation, analytical modeling, and analysis results on an ISS assembly mission.

14. SUBJECT TERMS	15. NUMBER OF PAGES
International Space Station; Electric power; Solar cells; Modeling	13
	16. PRICE CODE: A03

17. SECURITY CLASSIFICATION OF REPORT	18. SECURITY CLASSIFICATION OF THIS PAGE	19. SECURITY CLASSIFICATION OF ABSTRACT	20. LIMITATION OF ABSTRACT
Unclassified	Unclassified	Unclassified	